

## RESEARCH ARTICLE

# Handover Strategies for Emerging LEO, MEO, and HEO Satellite Networks

**ANDRA M. VOICU**<sup>ID</sup>, **ABHIPSHITO BHATTACHARYA**, AND **MARINA PETROVA**<sup>ID</sup>, (Member, IEEE)

Mobile Communications and Computing Group, RWTH Aachen University, 52072 Aachen, Germany

Corresponding author: Andra M. Voicu (voicu@mcc.rwth-aachen.de)

This work was supported in part by RWTH Aachen University through computing resources under Project thes0950 and Project rwth0767; and in part by the Federal Ministry of Education and Research of Germany (BMBF) through the Project "Open6GHub" under Grant 16KISK012.

**ABSTRACT** Satellite networks are expected to support global connectivity via future 3GPP non-terrestrial networks (NTNs), as well as private non-geostationary satellite orbit (NGSO) constellations, e.g. OneWeb, SpaceX, and Amazon's Kuiper. In both 3GPP and private NGSO networks, handling mobility is critical, due to the intrinsic continuous movement of the satellites. In this paper we select three representative inter-satellite handover (HO) strategies and we study their impact on the achievable space-to-ground link performance in emerging NGSO constellations. With 1) *Closest Satellite HO* a ground station always connects to the closest satellite, with 2) *Max Visibility HO* a ground station connects and remains connected to the satellite with the maximum visibility time, until this satellite stops being visible, while with 3) *CINR-based HO* a ground station is handed over to the closest satellite if the carrier-to-interference-and-noise ratio (CINR) decreases by 3 dB below a maximum reference level. The first two HO strategies achieve the upper and lower bounds of the satellite-to-ground link performance based on the constellation geometry, while the third one is representative of HO mechanisms triggered by signal strength measurements. We consider five private constellations with different characteristics, some of which have already been launched. The goal is to determine the most suitable HO strategy for each constellation and our results show that this depends on the constellation type, i.e. low earth orbit (LEO), medium earth orbit (MEO) and highly elliptical orbit (HEO), and design. For large LEO constellations with thousands of satellites like SpaceX and Kuiper, CINR-based HO is recommended, since it achieves a good tradeoff among the spectral efficiency, propagation delay and handover rate, while the Doppler shift is in any case high. For smaller LEO constellations with hundreds of satellites like OneWeb, Closest Satellite HO is preferred due to the highest spectral efficiency and lowest propagation delay, while the handover overhead is similar for all strategies. For MEO and HEO constellations with tens to a few hundreds of satellites like Mangata and Pleiades, Closest Satellite HO is best. This achieves the highest spectral efficiency, lowest delay and sometimes a low Doppler shift, while the handover rate is in any case low. Finally, CINR-based HO is recommended in seldom cases of strong inter-constellation interference. Overall, the results suggest that the inter-satellite HO strategy should be adjusted to the constellation specifics, where e.g. adaptive handover selection algorithms could be employed for constellations that are enhanced in time by adding new satellites and orbit types.

**INDEX TERMS** Handover, NGSO systems, satellite communications, space-terrestrial networks.

## I. INTRODUCTION

Satellite constellations will play a crucial role in providing ubiquitous connectivity as an integral part of emerging

The associate editor coordinating the review of this manuscript and approving it for publication was Mohamed M. A. Moustafa<sup>ID</sup>.

wireless networks. They could support a variety of services such as mobile broadband and fixed Internet connectivity for ground users in unserved and underserved areas, passengers on board of airplanes, as well as wireless connectivity for Internet-of-Things (IoT), tracking ships and their cargos, backhaul for ground base stations (BSs) or unmanned aerial

**TABLE 1.** New private NGSO constellations and their main satellite parameters in the downlink [4]. The constellations are proposed to operate in the same frequency bands, i.e. the Ku- (10.7–12.7 GHz downlink, 14.0–14.5 uplink), Ka- (17.8–19.7 GHz downlink, 27.5–30.0 GHz uplink), and V-band (37.5–42.0 GHz downlink, 47.2–51.4 GHz uplink) [5].

Constellation	Orbit type	Altitude [km]	No. satellites	Service & feeder channel width $B$ [MHz]	EIRPD max. [dBW/Hz]	Band	Started launch
Kepler	LEO (circular)	650	360	10, 100, 300, 500	-41.0	Ku, Ka	yes
Amazon's Kuiper	LEO (circular)	590–630	3236	100	-43.9	Ka	no
Mangata	MEO (circular)	6400	567	100, 500	-36.3	Ka, V	no
	HEO (elliptical)	perigee: >1200 apogee: <11600	224	100, 500	-36.3	Ka, V	
O3b	LEO (circular)	507	36	250, 260, 300, 500, 2500	-22.5	Ka	yes
	MEO (circular)	8062	76	250, 260, 300, 500, 2500	-22.5	Ka	
OneWeb Phase 1	LEO (circular)	1200	716	155, 250	-38.7	Ku, Ka	yes
OneWeb Phase 2	LEO (circular)	1200	47844	155, 250	-38.7	Ku, Ka	no
SpaceX	LEO (circular)	540–570	4408	50	-50.3	Ku, Ka	yes
SpaceX Gen2	LEO (circular)	328–614	30000	50, 100, 500, 800, 2000	-37.5	Ku, Ka	no
Telesat	LEO (circular)	1000–1325	1788	500, 800	-50.0	Ka	no
Viasat	LEO (circular)	1300	288	500, 800	-31.7	Ka, V	no
LeoSat	LEO (circular)	1400	84	400, 500	-45.0	Ka	no (shut down)
Karousel	geosynchronous (elliptical)	perigee: 31569 apogee: 40002	12	250	-22.7	Ku, Ka	no
New Spectrum Satellite's Pleiades	HEO (elliptical)	perigee: 1118 apogee: 26648	15	20, 25	-24.7	Ku, Ka	no
Space Norway	HEO (elliptical)	perigee: 8089 apogee: 43509	2	115, 250, 500, 1000	-26.0	Ku, Ka	no
Theia	LEO (elliptical)	perigee: 750 apogee: 809	120	1, 300, 400, 500, 1500	-43.5	Ku, Ka	no
AST&Science's SpaceMobile	LEO (elliptical)	perigee: >725 apogee: <740	243	500, 4500	-36.8	V	no
Boeing	LEO (circular)	1056	132	2000, 2500	-1.8	V	no
	HEO (elliptical)	perigee: >27354 apogee: <44222	15	2000, 2500	-1.8	V	

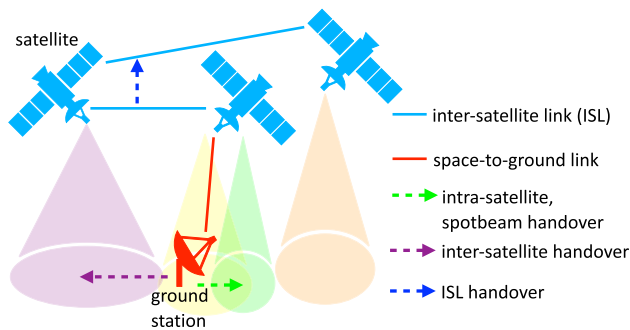


**FIGURE 1.** Illustration of handover types in satellites communications, as classified in [3]. A ground station and several satellites with different beams (purple, yellow, green, orange) are shown.

vehicles (UAVs) [1], [2]. Non-geostationary satellite orbit (NGSO) systems are especially suited for such applications, due to their lower communication delay and support for higher data rates at a lower transmit power compared to geostationary satellite orbit (GSO) systems. Nonetheless, NGSO communications systems also pose several challenges that need to be overcome.

Handling satellite mobility is one of the most critical aspects, due to the inherent movement of the satellites with respect to the Earth's surface. Other than in ground networks,

the area covered by an NGSO satellite moves continuously, so performing *inter-satellite* handovers is necessary to ensure continuous connectivity, even for fixed ground users. Fig. 1 illustrates inter-satellite handovers, alongside other handovers in satellite networks, i.e. intra-satellite spotbeam and inter-satellite link (ISL) handovers, as classified in [3]. Especially inter-satellite handovers are essential to enable continuous terrestrial connectivity. By contrast, spotbeam handovers target connectivity only within the coverage area of a given satellite and ISL handovers occur only for satellites supporting ISLs, which is an optional advanced feature.

The 3GPP standardization body is currently working on integrating GSO and NGSO satellites termed “non-terrestrial networks (NTNs)” in 5G-and-beyond cellular networks [6], [7]. Especially [6] addresses critical mobility aspects, but focuses on supporting handover control signalling and coping with the long propagation delay, rather than specifying HO strategies. Although some HO decision criteria are mentioned (i.e. based on measurements, location, timers, timing advance, and elevation angle), these solutions target primarily reducing the large control overhead when many users are present, rather than considering the user link performance. Also, quantitative performance evaluations of such HO decision criteria in real NGSO constellations are not presented. In the meanwhile, other private companies outside 3GPP have already planned, applied to the FCC in the U.S. for operation approval [4], and even started launching NGSO

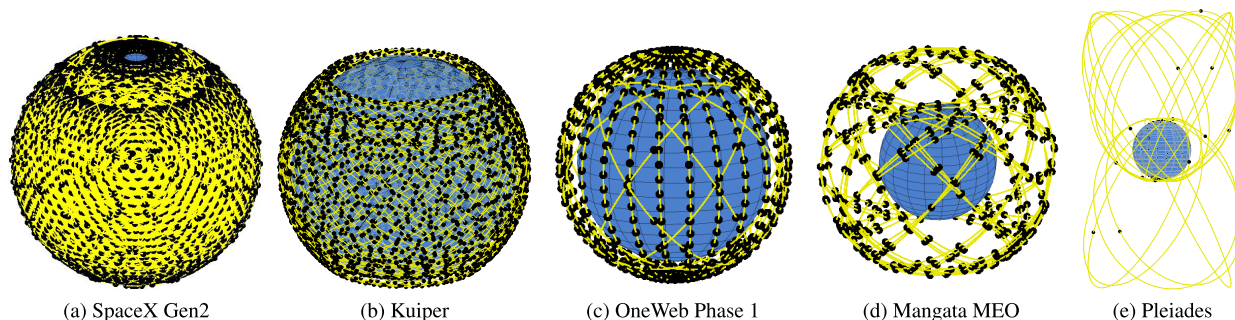


**FIGURE 2.** Examples of new private NGSO satellite constellations in the Ka-band, showing the Earth (blue), the satellite orbits (yellow), and the satellites (black). Table 1 summarizes the main design parameters of these constellations.

satellite constellations, e.g. OneWeb and SpaceX, *cf.* Table 1. However, the inter-satellite HO strategies implemented in such constellations are proprietary and their description is not publicly available.

As such, it is not yet understood which HO strategies should be selected for the emerging private and 3GPP NGSO constellations, so that a good space-to-ground link performance is achieved. This is especially important given the very different NGSO constellation designs and types, comprising low Earth orbit (LEO), medium Earth orbit (MEO), highly elliptical orbit (HEO), and geosynchronous constellations, as summarized for the private constellations in Table 1 and illustrated for some examples in Fig. 2. Furthermore, we believe that such constellation characteristics are relevant to future 3GPP NTN, which will likely build on existing state of the art. Although there is some prior work on satellite HO strategies in the literature, e.g. [8], [9], [10], [11], [12], [13], and [14], this considers either hypothetical constellations, or legacy constellations like Globalstar, namely small LEO constellations that do not reflect the very diverse emerging NGSO constellations.

The contributions of this paper are as follows.

- We select three representative satellite HO strategies from the literature and we are the first to study their impact on emerging NGSO constellations. With (i) *Closest Satellite HO* a ground station is always connected to the closest satellite, with (ii) *Max Visibility HO* the ground station connects to the satellite with maximum remaining visibility time and handovers occur only when this satellite goes out of visibility [8], while with (iii) *CINR-based HO* a ground station is handed over to the closest satellite, if its carrier-to-interference-and-noise ratio (CINR) is 3 dB lower than a reference maximum level. The first two HO strategies thus result in the upper and lower bounds of the satellite-to-ground link performance in terms of spectral efficiency, delay, handover rate, and Doppler shift. The third HO strategy is representative of HO mechanisms triggered by signal strength measurements, e.g. [6], and aims to avoid significant drops in spectral efficiency, while limiting the handover rate.
- Given the tradeoffs among the spectral efficiency, delay, handover rate, and Doppler shift, we determine the

most suitable HO strategies for five real private NGSO constellations in the Ka-band, that cover LEO, MEO, and HEO types (SpaceX Gen2 LEO, Kuiper LEO, OneWeb Phase 1 LEO, Mangata MEO, and Pleiades HEO).<sup>1</sup>

- To evaluate the space-to-ground link performance in terms of the metrics above, we conduct extensive simulations based on the MATLAB tool in [5] and [15], which we modify to incorporate the considered HO strategies and capture consecutive discrete moments in time. Furthermore, we consider a *standalone scenario* assuming interference mitigation among satellite constellations and also an *inter-constellation interference scenario*.

Our results show that the optimal HO strategy depends on the constellation type and design. For LEO constellations, CINR-based HO or Closest Satellite HO is preferred, depending on the constellation size, which determines a different tradeoff between the spectral efficiency, propagation delay and handover rate, while the Doppler shift is always high. By contrast, for MEO and HEO constellations with tens to a few hundreds of satellites like Mangata and Pleiades, Closest Satellite HO is always recommended. This improves the performance in terms of spectral efficiency, delay, and sometimes Doppler shift. Furthermore, CINR-based HO is useful in seldom cases of strong inter-constellation interference, but the target maximum CINR should be carefully chosen, depending on the atmospheric propagation conditions. These results suggest overall that the inter-satellite HO strategy should be selected based on the constellation design, where adaptive algorithms could be utilized for constellations that are frequently modified to include new orbits and satellites.

The rest of the paper is organized as follows. We first present the related work in Section II. In Section III we present the system model with the considered HO strategies and NGSO constellations, while Section IV describes

<sup>1</sup>We note that in this paper we focus on comparing the performance of different HO strategies among each other, for given NGSO constellations. Comparing the performance of different NGSO constellations against each other is outside the scope of this study, especially since the five considered constellations belong to distinct classes in terms of constellation geometry and size, so they were designed by their operators for different purposes.

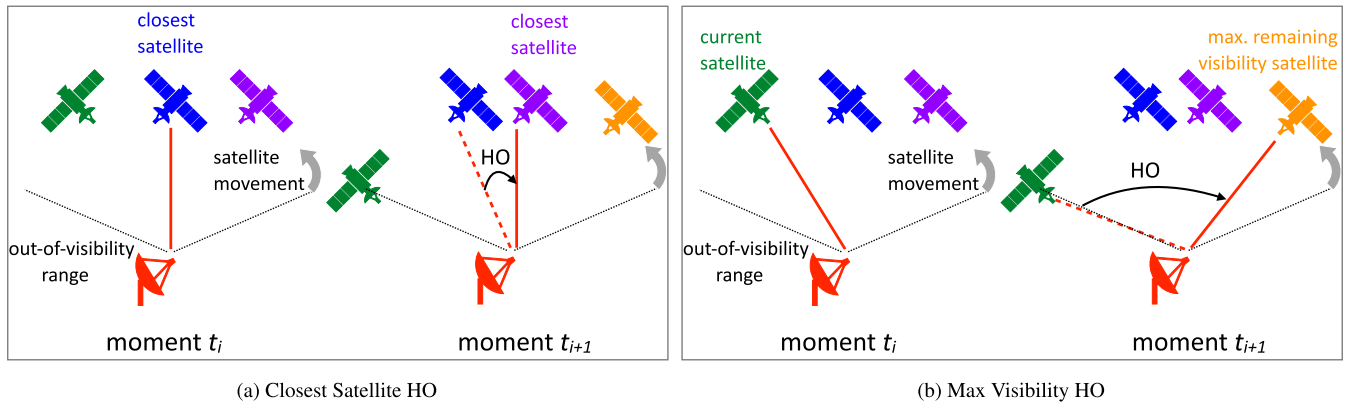


**FIGURE 3.** Illustration of two consecutive moments  $t_i$  and  $t_{i+1}$ , where a handover is executed according to (a) Closest Satellite HO and (b) Max Visibility HO. With Closest Satellite HO, the ground station is connected to the closest satellite (blue) at  $t_i$  and a handover is performed if another satellite becomes the closest (purple) at  $t_{i+1}$ . With Max Visibility HO, the ground station is connected at  $t_i$  to a satellite (green) that sometime prior to  $t_i$  was the maximum visibility satellite and remains connected to it until it is not visible anymore at  $t_{i+1}$ . Then the link is handed over to the next satellite that has the maximum remaining visibility time (orange).

the simulation tool and steps. We discuss our results and the impact of HO strategies on the space-to-ground link performance in Section V. Section VI concludes the paper.

## II. RELATED WORK

Prior work on handovers in NGSO satellite communications has addressed 3GPP technologies, e.g. [16] and [17], or adopted a more general perspective, e.g. [8], [9], [10], [11], [12], [13], and [14]. Handover control signalling issues were identified for LTE [16] and 5G NR [17], due to satellite mobility, the large cell footprints covering many users and sometimes different countries and regulatory areas, as well as long propagation delay potentially resulting in long service interruptions. Some solutions were suggested, namely handover execution at different protocol layers [16] and different handover triggering criteria (location based, maximum timing advance to target cell, absolute time, or timer based) that avoid simultaneous handovers of many users [17]. However, these solutions aim at limiting the control overhead and are not complete HO strategies defining also how the next satellite is selected. Furthermore, they are not quantitatively evaluated and the perspective of the user link performance is largely missing. By contrast, we take a complementary approach where we select three representative HO strategies from the literature and we quantitatively and comprehensively evaluate the space-to-ground link performance in terms of spectral efficiency, delay, HO rate, and Doppler shift.

There exist early works on HO strategies based on e.g. the maximum service time, maximum number of free channels, minimum distance [8], Doppler shift [9], or dual satellite diversity in case of critical channel conditions [10]. However, these works were conducted prior to the recent developments with the private satellite operators, so they considered only hypothetical or small legacy LEO constellations like

Globalstar, Teledesic, and Iridium. Thus, it is not obvious what the effect of such HO strategies is, if employed in the today's emerging LEO, MEO, and HEO constellations. Furthermore, obsolete performance metrics such as the call blocking probability were sometimes considered, which characterize legacy circuit-switched networks but not contemporary packet-based networks where the throughput and delay are relevant.

Recent works proposed more sophisticated handover algorithms for e.g. determining handover sequences that reduce the control overhead [11], incorporating satellites in a software-defined network (SDN) [12], load-balancing with machine learning (ML) [13], and a user-centric approach buffering user data in multiple satellites [14]. Also these works considered only the legacy Globalstar LEO constellation [11], or simplistic hypothetical LEO [12], [14] and MEO constellations [13] with only tens to at most 200 satellites, so a fundamental understanding of how basic HO strategies affect the link performance of emerging NGSO constellations of different orbit types and various sizes of up to thousands of satellites is missing. We note that there are some works in the literature that consider emerging NGSO constellations, however, they focus on aspects other than handovers, e.g. inter-constellation interference [5], [15] and routing in the satellite networks [18].

In this paper we thus comprehensively study the space-to-ground link performance for two basic HO strategies based on constellation geometry, from the literature, i.e. closest satellite and maximum remaining visibility satellite [8],<sup>2</sup> and an additional HO strategy based on measured CINR level, for five real diverse emerging NGSO constellations. Based on these HO strategies we obtain the upper and lower

<sup>2</sup>We note that the closest satellite-based handovers are equivalent to the maximum elevation criterion for circular LEO and MEO constellations, but not for HEO geometries. Furthermore, the maximum remaining visibility criterion is sometimes termed in the literature as the maximum service time criterion.

bounds and also intermediate tradeoff values of the spectral efficiency, propagation delay, HO rate, and Doppler shift and we recommend suitable HO strategies for each constellation type.

### III. SYSTEM MODEL & PARAMETERS

This section presents the system model, where there is a ground station that connects to one satellite at a time, from a given NGSO constellation. As the satellite that the ground station connects to moves along its orbit and the space-to-ground link performance degrades, handovers are performed to maintain connectivity, for downlink transmissions from the satellite to the ground station. The remainder of this section presents the considered HO strategies according to which the ground station successively connects to satellites, in Section III-A. The simulation scenarios are presented in Section III-B. The considered satellite constellations with the satellite transmitter parameters are summarized in Section III-C, and the ground station receivers with their antenna parameters and locations are presented in Section III-D.

#### A. HO STRATEGIES

We select two representative HO strategies based on the geometry of satellite networks [8]: (i) *Closest Satellite HO*, where the ground station always connects to the closest satellite; and (ii) *Max Visibility HO*, where the ground station connects to the satellite with the maximum remaining visibility time and remains connected to this satellite until it exits the visibility range. This range is defined as the satellite elevation angle  $\phi$  being above a minimum elevation angle  $\phi_{min}$  and these two HO strategies are illustrated in Fig. 3. We then select a third HO strategy, representative of signal strength measurement based handovers, namely (iii) *CINR-based HO*, where a ground station is handed over to the closest satellite, if the carrier-to-interference-and-noise ratio  $CINR$  at the ground station decreases by a margin  $\gamma$  below a reference  $CINR_{max}$ . We define this reference as the average  $\overline{CINR}$  of Closest Satellite HO over a satellite orbital period, since Closest Satellite HO achieves the maximum  $CINR$  at each moment in time. We set  $\gamma=3$  dB as an example where only a rather small degradation of the link quality is tolerated.

We note that Closest Satellite HO aims at minimizing the path loss and propagation delay, but maximizes the number of handovers and thus the associated overhead. By contrast, Max Visibility HO aims to minimize the number of handovers, but may lead to higher path losses and propagation delays. Consequently, these HO strategies result in the upper and lower bounds of the link performance with respect to spectral efficiency, propagation delay, and handover rate. By contrast, CINR-based HO takes into account explicitly the space-to-ground link conditions, rather than the constellation geometry as done by Closest Satellite HO and Max Visibility HO, and aims to avoid a major decrease in the spectral efficiency. At the same time, it aims to avoid an excessive number of handovers.

TABLE 2. Summary of considered HO strategies.

Description HO strategy	Handover triggering condition	Next serving satellite to be handed over to
Closest Satellite HO	closest satellite is different than current one (or $\phi < \phi_{min}$ )	closest satellite (out of visible ones)
Max Visibility HO	current satellite goes out of visibility ( $\phi < \phi_{min}$ )	satellite with longest remaining visibility time
CINR-based HO	$CINR < CINR_{max} - \gamma$ (or $\phi < \phi_{min}$ )	closest satellite (out of visible ones)

The three considered HO strategies are summarized in Table 2 and, for all of them, a link can be established and maintained only with visible satellites, i.e. if  $\phi \geq \phi_{min}$ . We note that in this paper we assume that handovers are performed in an ideal way, namely as soon as the handover decision criterion is fulfilled and without any additional delay due to control signalling. This would correspond in practice to the case where the connection to the next satellite is initiated before reaching the moment to release the current connection. This could be achieved with signalling between satellites, e.g. using ISLs.

#### B. SCENARIOS

We assume downlink transmissions from the satellite to the ground station and we consider two scenarios: (i) *standalone scenario* where the constellations do not interfere with each other; and (ii) *inter-constellation interference scenario* where there is interference from other constellations. The standalone scenario corresponds to the case where interference mitigation techniques are used among constellations, e.g. each constellation operates on different channels than those used by other constellations covering the same ground area (cf. band-splitting mandated by the FCC in the US [5]).

For the inter-constellation interference scenario, we assume the worst-case interference where all other NGSO constellations that can use the same channel simultaneously cause interference to the ground station (connected to a serving satellite in a constellation of interest). For this, we assume a single interfering satellite from each interfering constellation, where this satellite is selected from its constellation to be the closest to the serving satellite that is forming a link to the ground station. The serving satellite is selected, in turn, based on the HO strategies in Section III-A. We thus assume the highest NGSO-NGSO interference levels, since the ground station beamforms in the direction of the serving satellite, which is close to the direction of the selected interfering satellites, resulting in the highest likelihood that downlink interference is captured through the main antenna lobe of the ground station. Furthermore, the interfering satellite also beamforms towards the victim ground station. Finally, we note that we do not model intra-constellation interference, since this can be managed in a straightforward way by each

**TABLE 3.** Considered private NGSO constellations and parameters in the downlink, for the Ka-band [4].

Const.	Satellite			Ground station		
	$EIRPD$ [dBW/Hz]	Estimated $v$ [km/s]	$\phi_{min}$ [°]	$G_{RX}$ [dBi]	$D$ [m]	$T$ [K]
SpaceX Gen2	-42.4	7.7	25	48.3	0.48	200
Kuiper	-43.9	7.540	35	38	0.45	200
OneWeb Phase 1	-52.0	7.260	55	50	1.80	200
Mangata MEO	-43.3	5.586	20	50	1.80	200
Pleiades	-30.3	min: 2.11 max: 6.40	25	60.4	6	110

satellite operator individually. Also, we do not model any interference from/to GSO satellites in our simulations. This could also affect the HO strategy choice for NGSO satellites, either to avoid strong interference from GSO satellites, or to protect the GSO satellites from interference, in Ka sub-bands where NGSO satellites are required to avoid interference to GSO systems [5].

### C. SATELLITE CONSTELLATIONS

We evaluate the impact of the considered HO strategies on the space-to-ground link of five example constellations set to operate in the Ka-band, i.e. SpaceX Gen2, Kuiper, OneWeb Phase 1, Mangata MEO, and Pleiades [4]. We select these NGSO constellations due to their very different design properties, as shown in Fig. 2 and summarized in Table 1. Due to the different altitudes and orbit geometries resulting in different satellite velocities, as well as the different constellations sizes, these constellations cover a wide range of operation points, as follows.

SpaceX Gen2, Kuiper and OneWeb Phase 1 are all LEO constellations, so their satellite velocities are high and comparable. The velocity  $v$  is summarized in Table 3, as estimated based on orbital mechanics [5]. We thus expect that handovers are required frequently. However, SpaceX Gen2 and Kuiper are much larger constellations and comprise only inclined orbits, compared with OneWeb Phase 1 which is smaller and has mostly polar orbits. As such, the number of available satellites to hand the link over to is different. Mangata MEO and Pleiades HEO have higher altitudes versus the LEO constellations and therefore also lower velocities, so fewer handovers are required. For HEO orbits, the visibility time of a satellite is prolonged additionally when the satellite is close to the apogee. In particular, Pleiades satellites are active only above 17118 km altitude, where the velocity is in the lower range. Note that at every simulated instance, the velocity is calculated based on the satellite location on the orbit. Furthermore, due to the smaller sizes of Mangata MEO and Pleiades, there are fewer satellites to select from, when handovers are performed.

We assume transmissions in the Ka-band with a carrier frequency  $f_c=19$  GHz. The corresponding maximum  $EIRPD$  of these constellations specified for this band and  $\phi_{min}$  [4]

are summarized in Table 3. For the inter-constellation interference scenario, we consider a channel where most NGSO constellations in the Ka-band can operate according to [5], in order to obtain the highest number of interferers and thus the worst-case interference. Thus, each of the constellations above is interfered by all the other considered constellations, except Pleiades which does not operate over the assumed channel, and also by seven other constellations that can all operate on an overlapping channel (Kepler, LeoSat, O3b, Telesat, Theia, Karousel, Mangata HEO). Further characteristics of these seven constellations are summarized in Table 1. Thus, for each considered constellation (except Pleiades) there are  $N=10$  interfering constellations.

### D. GROUND STATIONS

We assume a static ground station located in Aachen, Germany. This ground station connects to a given NGSO constellation and receives traffic in the downlink. The receiver is characterized by the maximum receive gain  $G_{RX}$ , as summarized in Table 3, where the ground station is a gateway for Pleiades and a user terminal for all other considered constellations. We note that there is currently only limited information about the ground receiver parameters of each considered constellation, where  $G_{RX}$  is typically not explicitly specified. As such, we estimate

$$G_{RX} = A_{eff} \times \left( \frac{\pi D f_c}{c} \right)^2, \quad (1)$$

where  $A_{eff}$  is the antenna efficiency equal to 0.8 [5],  $D$  is the antenna diameter, and  $c$  is the speed of light. Term  $D$  and the ground station noise temperature  $T$  are specified by each operator in [4] and are summarized in Table 3.<sup>3</sup>

We emphasize that the antenna parameters  $EIRPD$  and  $G_{RX}$  in Table 3 refer to the main antenna lobes of the satellite and ground station, respectively. In this paper we assume that the transmitter and receiver are always beamformed towards each other, so the main antenna lobes are pointing in the direction of the line-of-sight (LOS) path. This corresponds to a so called *Earth fixed cell* configuration for the satellites, where a satellite attempts to cover a fixed area on the ground by beamforming towards it, for as long as possible [3].

The interfering satellites are also beamformed towards the victim ground station. However, the victim ground station is beamformed towards the serving satellite, so interference is not received from the direction of its main lobe. For this, the considered ground station antenna pattern is based on the ITU-R recommendations in [5] and [19].

## IV. SIMULATION TOOL AND STEPS

### A. SIMULATION TOOL

For this study we adopted the MATLAB satellite simulator in [5] and [15] and we modified it to support inter-satellite

<sup>3</sup>Note that the SNR of the satellite-to-ground links may be different in bands other than the Ka-band, if the same satellite and ground station parameters are specified by the operator.

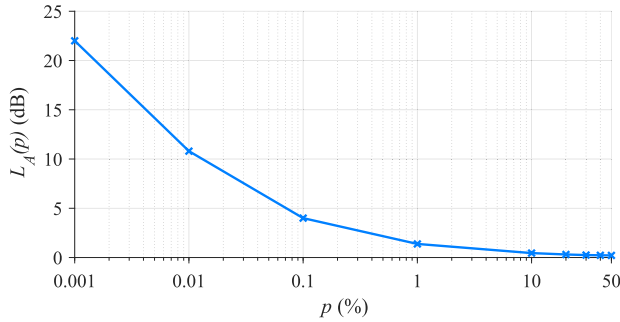


FIGURE 4. Example atmospheric attenuation  $L_A(p)$  for the possible range of unavailability probability  $p$ , for a ground station in Aachen, Germany.

handovers. The simulator in [5] and [15] was originally developed to model the impact of inter-constellation interference and interference mitigation techniques on the satellite-to-ground link CINR and spectral efficiency. The simulator comprehensively takes into account different constellation types (LEO, MEO, HEO), sizes, and geometric orbit properties to compute real positions of the satellites in their orbits, at random moments in time. Additionally, it incorporates the Earth rotation and can model any real Earth location for the ground stations, which has an impact on the elevation angles and distances at which the satellites appear and also on the atmospheric conditions. Furthermore, it incorporates satellite and ground station transceiver parameters, antenna patterns, beamforming properties (i.e. direction and off-boresight losses), and atmospheric attenuation to accurately model the link CINR and spectral efficiency for static ground stations.

We thus adopted this simulator to realistically model the constellations, ground station, and link metrics above and we further significantly modified it to support inter-satellite handovers. To this end we first introduced modifications that allow computation of the satellite locations with respect to given Earth ground locations at consecutive discrete moments in time, spaced at configurable fixed intervals  $\Delta t$ . This enables us to verify when and how often the triggering conditions for a handover occur. Furthermore, we incorporated the three considered HO strategies in Section III, with their specific triggering conditions and criteria to select the next serving satellite. Finally, we modified the simulator to compute the additional metrics of one-way propagation delay, Doppler shift, and handover rate for the space-to-ground link. The simulation steps are presented in detail in Section IV-B.

### B. SIMULATION STEPS

We conducted extensive simulations for a total simulated duration of 10,000 s. We simulate consecutive moments of time  $t_i$  at intervals of  $\Delta t=1$  s and for each of them the following steps are performed.

#### STEP 1

Take as input the time moment  $t_i$ , a given HO strategy, and a considered satellite constellation. If the inter-constellation

TABLE 4. Considered  $CINR_{max}$  values used for the triggering condition of CINR-based HO.

Scenario	Constellation	$CINR_{max}$ [dB]
standalone (high atmospheric attenuation $p=0.001\%$ )	SpaceX Gen2	6.1
	Kuiper	3.35
	OneWeb Phase 1	0.8512
inter-constellation interference (low atmospheric attenuation $p=50\%$ )	SpaceX Gen2	26
	Kuiper	24.3
	OneWeb Phase 1	21.65

interference scenario is considered, assume additionally the interfering constellations.

#### STEP 2

Calculate the positions of all satellites in the considered (and, if applicable, interfering) constellation with respect to Earth at  $t_i$ , assuming the relevant constellation geometry in Table 1.

#### STEP 3

Determine all satellites that are visible to the ground station located in Aachen. The visible satellites appear for the ground station above  $\phi_{min}$ , summarized for each constellation in Table 3.

#### STEP 4

For the current serving satellite, estimate  $\phi$  and the carrier-to-noise-and-interference ratio  $CINR$ . For the standalone scenario,  $CINR$  is in fact equal to the carrier-to-noise ratio

$$CINR = EIRPD - PL - L_A(p) + G_{RX} - 10\log(Tk), \quad (2)$$

where  $EIRPD$  is given for the satellites of each considered constellation in Table 3 and is first adjusted for off-boresight losses [5],  $PL$  is the free-space path loss,  $L_A(p)$  is the atmospheric attenuation depending on unavailability probability  $p$ ,  $G_{RX}$  and  $T$  are summarized for the ground station in Table 3, and  $k$  is the Boltzmann constant. The atmospheric attenuation  $L_A(p)$  is modelled based on the ITU-R model in [20], as implemented in [21], where we consider two values of  $p$ : (i)  $p=50\%$  corresponding to the lowest atmospheric attenuation; and (ii)  $p=0.001\%$  corresponding to the highest atmospheric attenuation, cf. Fig. 4.

For the inter-constellation interference scenario,

$$CINR = EIRPD - PL - L_A(p) + G_{RX} - 10\log\left(Tk + \sum_{n=1}^N I_n\right), \quad (3)$$

where  $I_n$  is the interference from each selected interfering satellite  $n$ , of each of the  $N=10$  interfering constellations. We estimate

$$I_n = 10^{(EIRPD_n - PL_n - L_{A,n}(p) + G_{RX,n})/10}, \quad (4)$$

where  $EIRPD_n$  is the  $EIRPD$  for the constellation that the interfering satellite  $n$  belongs to,  $PL_n$  is the free space path loss between the interfering satellite  $n$  and the ground station,  $L_{A,n}(p)$  is the atmospheric attenuation between the interfering

satellite  $n$  and the ground station, and  $G_{RX,n}$  is the ground station receive antenna gain in the direction of the interfering satellite  $n$ .

#### STEP 5

Verify whether the handover triggering condition for the selected HO strategy is fulfilled, as presented in Section III-A. If required, hand over the link to a new visible satellite and update  $CINR$ . For CINR-based HO, we consider only LEO constellations and we assume the  $CINR_{max}$  values summarized in Table 4. These values represent the  $CINR$  obtained with the Closest Satellite HO and averaged over the satellite orbital period of each respective constellation. We note that for the considered MEO and HEO constellations we show in Section V-A that Closest Satellite HO is preferred in the standalone scenario, so CINR-based HO would not bring any benefit. Consequently, for brevity, we omit results for CINR-based HO for Mangata MEO and Pleiades HEO.

#### STEP 6

Estimate the space-to-ground link performance evaluation metrics, for the link between the ground station and the serving satellite. These metrics are the spectral efficiency  $SE$ , one-way propagation delay  $t_{prop}$ , and Doppler shift  $f_d$ .<sup>4</sup> We obtain  $SE$  by directly mapping  $CNR$  to it, based on the DVB-S2X standard [22]. Term  $t_{prop} = d/c$ , where  $d$  is the distance between the ground station and the satellite that it is connected to. Finally,  $f_d = (v_r f_c \cos(\alpha))/c$  assumes the relative speed between the satellite and ground station  $v_r$ , where the satellite is mobile and the ground station is fixed on the ground, but moves together with the Earth rotation, and  $\alpha$  is the angle between the satellite movement direction and the direction of the link to the ground station.

Next, Steps 2–6 are repeated for each consecutive moment  $t_{i+1}$ , until the end of the simulated time. Finally, the link performance in terms of handover rate  $\rho_{HO}$  is estimated by simply dividing the total number of handovers performed in Step 5 by the simulated duration of 10,000 s. We note that, in a future step, the metrics  $SE$  and  $\rho_{HO}$  could be incorporated in a long-term average throughput metric, to take into account more specifically the handover overhead impact, if the details of the protocol stack above the Physical Layer are known (e.g. handover interruption time). Throughout this paper we quantify the handover overhead in terms of  $\rho_{HO}$  only, since the specifics of the proprietary protocols of the private NGSO constellations are not available.

## V. RESULTS

In this section we present and discuss our simulation results showing the impact of the considered HO strategies on the space-to-ground link, in terms of the metrics  $SE$ ,  $t_{prop}$ ,  $\rho_{HO}$ , and  $f_d$ , as defined in Section IV-B. We first present the

results for the standalone scenario in Section V-A and then for the inter-constellation interference scenario in Section V-B. In Section V-C we summarize our findings and discuss further related aspects.

### A. STANDALONE SCENARIO

#### 1) LEO CONSTELLATIONS

##### SPECTRAL EFFICIENCY

Fig. 5 shows the link spectral efficiency  $SE$ , propagation delay  $t_i$ , and Doppler shift  $|f_d|$ , over part of the simulated time, for the considered LEO satellite constellations and all HO strategies. Let us first focus on  $SE$  in Fig. 5, which is shown for a low and a high atmospheric attenuation. For a low atmospheric attenuation ( $p=50\%$ ), with the Closest Satellite HO, the spectral efficiency of all LEO constellations is constant and reaches 6 bps/Hz, i.e. the maximum possible with the DVB-S2X standard. For Max Visibility HO, SpaceX and Kuiper suffer from drops of down to 3.8 and 5.1 bps/Hz, respectively. These drops correspond to satellite positions in the proximity of the minimum elevation angle  $\phi_{min}$ , where the distance between the satellite and the ground station is the largest in LEO constellations. For these positions, the EIRPD levels of SpaceX and Kuiper are not high enough to fully compensate for the path loss. Nonetheless, we consider these effects to be sporadic and minor. Since Max Visibility HO results in the lower-bound  $SE$  and the lower bound is overall close to the upper bound for the considered LEO satellites, the choice of HO strategy does not significantly affect the spectral efficiency when the atmospheric attenuation is low.

Let us now consider the example of a less likely high atmospheric attenuation ( $p=0.001\%$ ) in Fig. 5. We note that  $SE$  is overall significantly lower than that for a low atmospheric attenuation, for all considered constellations, regardless of the HO strategy. This shows that none of the HO strategies can fully compensate for the high loss caused by extreme atmospheric conditions. However, for SpaceX Gen2 and Kuiper,  $SE$  for Closest Satellite HO is significantly higher (by up to 1.3 and 3 bps/Hz, respectively) than for Max Visibility Satellite HO. Furthermore, CINR-based HO often achieves a similar  $SE$  as Closest Satellite HO, for these two constellations. The  $SE$  for OneWeb is also highest with Closest Satellite HO, but the other HO strategies often achieve a similar  $SE$ . This is due to the fewer satellites comprised by OneWeb, which result in overall fewer opportunities to perform a HO and fewer satellites to select a new serving satellite from. Overall, the results in Fig. 5 show that, for LEO constellations, the HO strategy does not have a significant impact on  $SE$ , except for less likely cases of extremely high atmospheric attenuation; in such cases the Closest Satellite HO is preferred.

##### PROPAGATION DELAY & HO RATE

Fig. 5(b) shows the one-way propagation delay  $t_{prop}$  of the space-to-ground links, alongside the moments when

<sup>4</sup>End-to-end metrics are outside the scope of this paper, but are relevant to the system performance. For instance, routing between two ground end points via multiple space-to-ground links may result in a much longer end-to-end delay compared to the one-way link propagation delay.



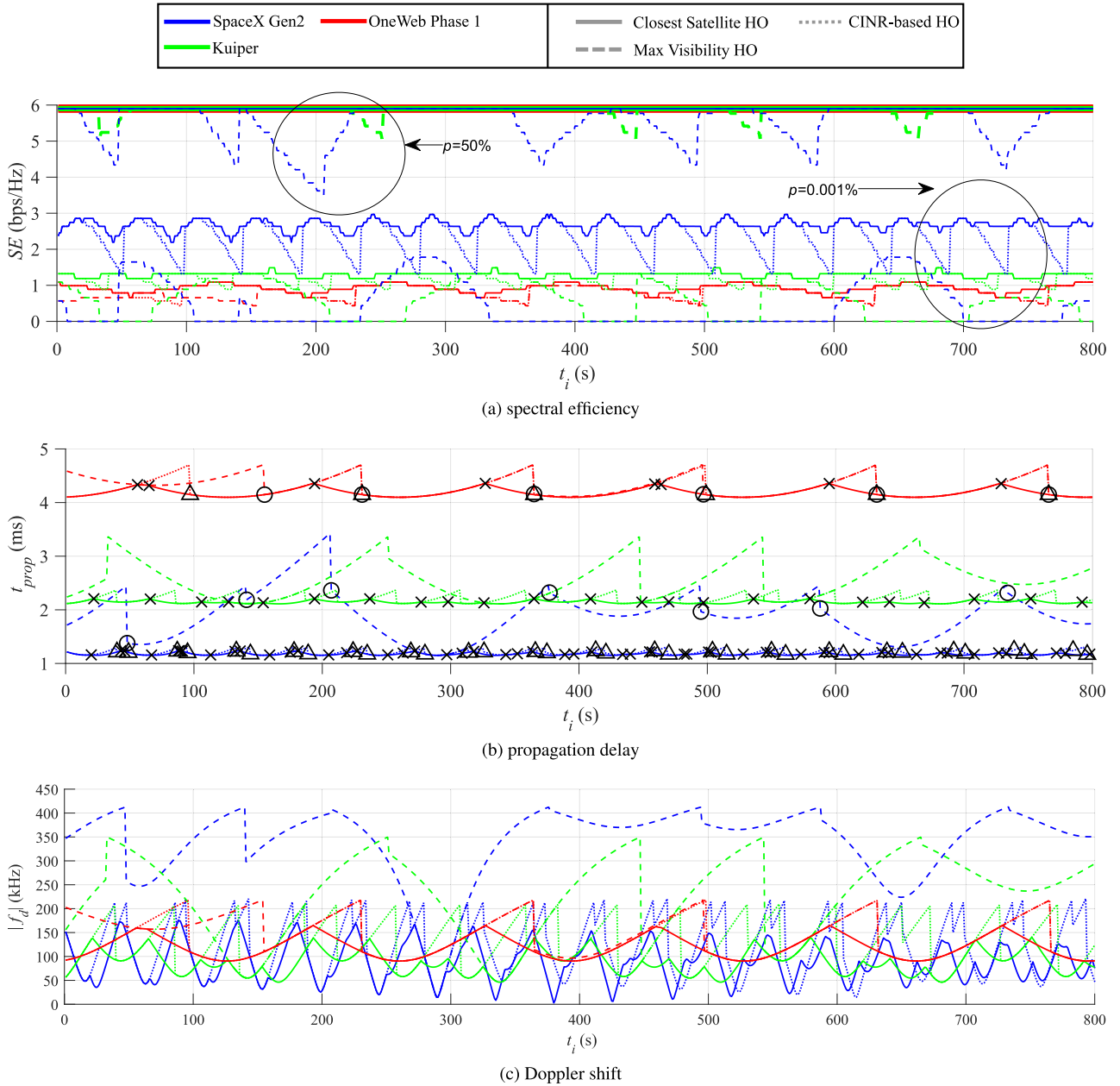


**FIGURE 5.** Results for the standalone scenario, for the considered LEO constellations, for different HO strategies, over part of the simulated time  $t_i$ : (a) spectral efficiency  $SE$ , (b) propagation delay  $t_{prop}$ , and (c) Doppler shift in absolute value  $|f_d|$ . The  $SE$  is shown for a low ( $p=50\%$ ) and a high ( $p=0.001\%$ ) atmospheric attenuation. For  $t_{prop}$ , the time instances when handovers are performed are marked for Closest Satellite HO ( $\times$ ), Max Visibility HO ( $\circ$ ), and CINR-based HO ( $\Delta$ ). The handovers for Closest Satellite HO and Max Visibility HO are the same regardless of the atmospheric attenuation. The handovers for CINR-based HO are shown only for  $p=0.001\%$ .

handovers occur, for all considered LEO constellations. We note that these results correspond to the  $SE$  shown in Fig. 5(a) for a high and low atmospheric attenuation. For Closest Satellite HO and Max Visibility HO,  $t_{prop}$  and the handover moments do not depend on the atmospheric attenuation (or the path loss in general), but only on the constellation geometry and satellite positions, so the corresponding results in Fig. 5(b) hold for any atmospheric attenuation. For CINR-based HO, the selection of the serving satellites and thus  $t_{prop}$  and handover moments depend

on the atmospheric attenuation; we show these results for  $p=0.001\%$ .

The propagation delay for LEO constellations in Fig. 5(b) reflects the height of the constellations. SpaceX Gen2 achieves overall the lowest delay, corresponding to its low altitude. However, the delay varies significantly with the HO strategy, where Closest Satellite HO and CINR-based HO achieve a delay of at most 1.3 ms, whereas Max Visibility HO can introduce up to 3.4 ms delay. This is due to the low  $\phi_{min}$  of SpaceX, which allows Max Visibility HO to keep the ground

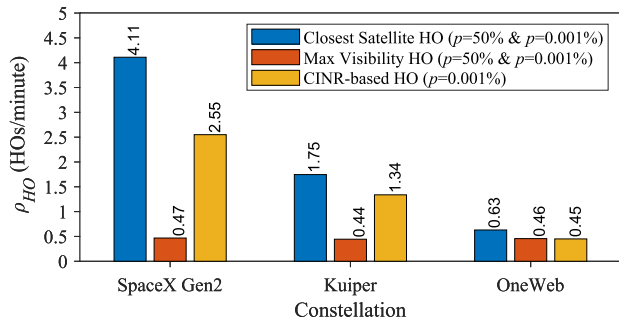


**FIGURE 6.** Average handover rate  $\rho_{HO}$  for the standalone scenario and all HO strategies, for the considered LEO constellations.

station connected to a serving satellite at low elevation angles. Consequently, only Closest Satellite HO and CINR-based HO are suitable for SpaceX. However, these two strategies also introduce many handovers. We show the handover rate  $\rho_{HO}$  explicitly in Fig. 6. We observe that  $\rho_{HO}$  is rather high for SpaceX with Closest Satellite HO, due to the large number of satellites, but is significantly decreased with CINR-based HO. Consequently, CINR-based HO achieves a good tradeoff among  $SE$ ,  $t_{prop}$ , and  $\rho_{HO}$  for SpaceX Gen2.

The propagation delay for Kuiper in Fig. 5(b) shows a similar trend as for SpaceX Gen2, where Max Visibility HO introduces a significantly longer delay compared to Closest Satellite HO and CINR-based HO. However, the handover rate for Kuiper in Fig. 6 is similar for Closest Satellite HO and CINR-based HO, unlike for SpaceX Gen2.

The delay for OneWeb Phase 1 in Fig. 5(b) shows a somewhat small difference among HO strategies, since OneWeb has fewer satellites than SpaceX Gen2 and Kuiper, so there are not many opportunities to select a new closest satellite with Closest Satellite HO. Nonetheless, Closest Satellite HO sometimes achieves an up to 0.5 ms shorter delay than the other two HO strategies. Furthermore, Fig. 6 shows that there is only a minor difference in the handover rate among the HO strategies for OneWeb Phase 1, so Closest Satellite HO is then preferred, due the shorter propagation delay.

#### DOPPLER SHIFT

Fig. 5(c) shows the Doppler shift in absolute value  $|f_d|$ .<sup>5</sup> For SpaceX Gen2 we observe the largest overall variation of  $f_d$  (from 0 to 410 kHz), due to the high velocity of the satellites and the large range of angles  $\alpha$  between the movement direction and the direct path to the ground station. Thus, the Doppler shift is significant and should be compensated for. As an insight, the range of  $f_d$  is different for the three HO strategies, namely up to 160 kHz (8.42 ppm), 210 kHz (11.05 ppm), and 410 kHz (21.57 ppm) for Closest Satellite HO, CINR-based HO, and Max Visibility HO, respectively. Nonetheless, all these  $f_d$  ranges are larger than expected and tolerated in ground deployments, e.g. up to

<sup>5</sup>In the rest of the paper we use the notation  $f_d$  instead of  $|f_d|$ , for simplicity.

950 Hz in terrestrial LTE [16], so they require specific compensation solutions. Such efficient solutions are expected to exist in practice, given that 3GPP foresees even larger NTN Doppler shift values of up to 24 ppm that can be significantly compensated for, so that the Doppler shift can be reduced down to 0.42 ppm [6]. These observations hold also for Kuiper, although the specific Doppler shift values are different and reach at most 350 kHz.

For OneWeb we observe similar effects, where the Doppler shift is also large. However, it varies over a similar range for all HO strategies, i.e. between 92 and 222 kHz, unlike for SpaceX Gen2 and Kuiper. This is consistent with the predominantly polar orbits of OneWeb, where  $\alpha$  can take only a limited range of values, whereas SpaceX Gen2 and Kuiper have more orbits than OneWeb, that are also inclined at different angles.

#### SUMMARY

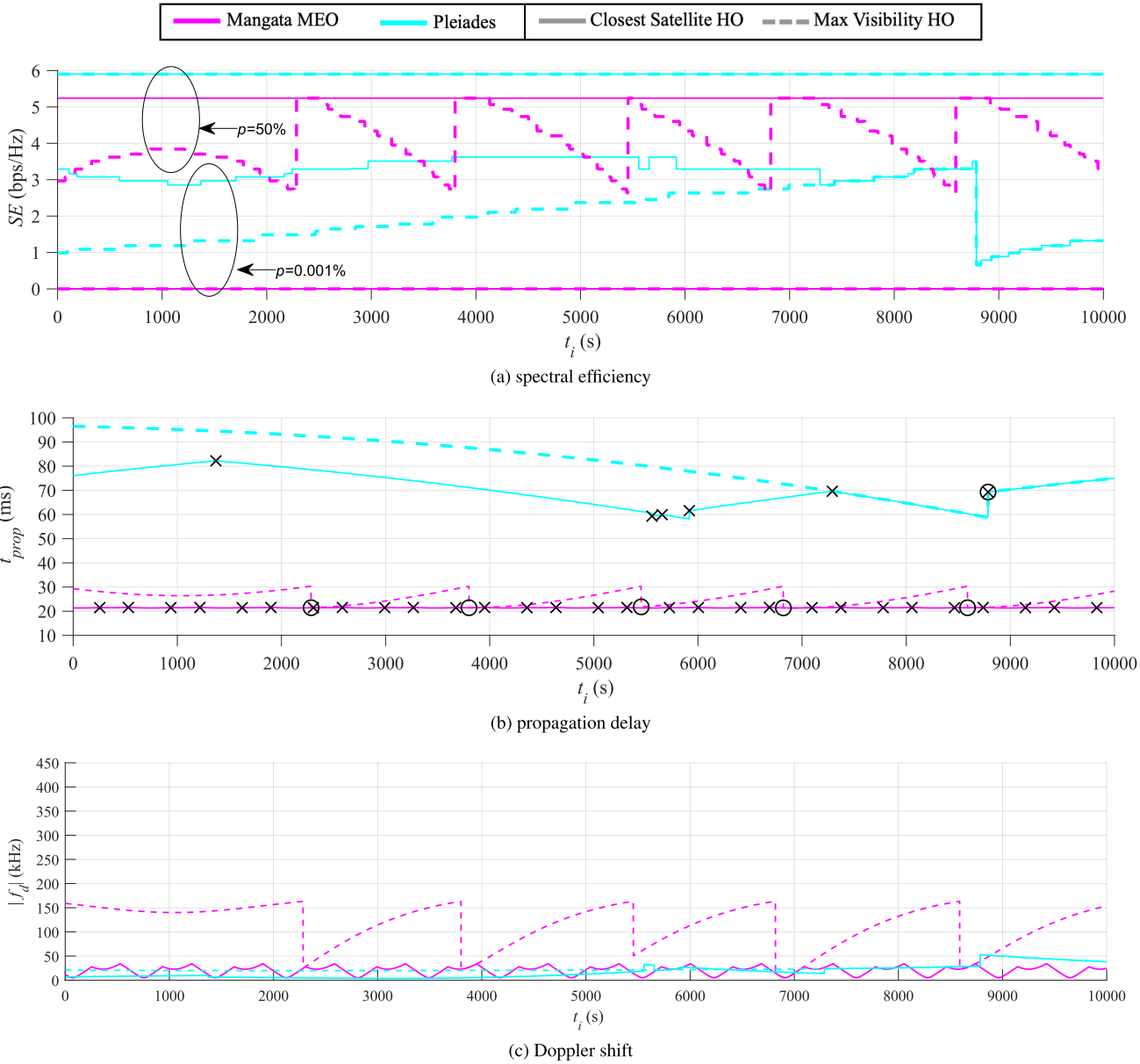
Overall, CINR-based HO is preferred for large LEO constellations like SpaceX and Kuiper, since it achieves a good tradeoff among  $SE$ , delay, and HO rate, while solutions to compensate the high Doppler shift are needed in any case. For smaller LEO constellations like OneWeb, Closest Satellite HO is preferred, since it achieves the highest  $SE$  and shortest delay, while increasing the handover control overhead only marginally. As for the large LEO constellations, none of the HO strategies has a significantly different impact on the Doppler shift and solutions are needed in any case to compensate for the high Doppler shift.

## 2) MEO & HEO CONSTELLATIONS

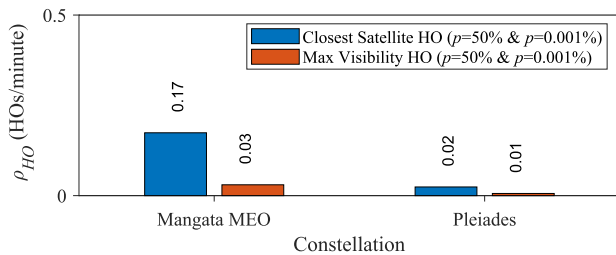
### SPECTRAL EFFICIENCY

Fig. 7 shows the link spectral efficiency  $SE$ , propagation delay  $t_i$ , and Doppler shift  $|f_d|$ , over the simulated time, for the considered MEO and HEO satellite constellations (Mangata MEO and Pleiades) and different HO strategies. The  $SE$  for a low atmospheric attenuation ( $p=50\%$ ) in Fig. 7 varies from 2.8 to 5.2 bps/Hz and is 5.9 bps/Hz for Mangata MEO and Pleiades, respectively. The latest transceiver parameters of Pleiades thus compensate fully for the large path loss caused by the satellite-to-ground distance, different than the initial transceiver parameters considered in prior work [23]. Furthermore, both HO strategies are equally good to achieve the highest spectral efficiency for Pleiades, if the atmospheric attenuation is low. For Mangata MEO, the path loss is not fully compensated for, due to the rather high altitude and jointly with the rather low satellite  $EIRPD$  (cf. Table 3). Consequently, Closest Satellite HO is the preferred HO strategy for Mangata, since it achieves a constant  $SE$  that is often up to 2.4 bps/Hz higher than that for Max Visibility HO.

Let us now consider an example of a less likely high atmospheric attenuation ( $p=0.001\%$ ) in Fig. 7. The  $SE$  for Pleiades varies overall between 0.7 and 3.5 bps/Hz, where Closest Satellite HO achieves up to 2.3 bps/Hz more than Max Visibility HO. Mangata MEO cannot establish any satellite-



**FIGURE 7.** Results for the standalone scenario, for the considered MEO and HEO constellations, for different HO strategies, over the simulated time  $t_i$ : (a) spectral efficiency  $SE$ , (b) propagation delay  $t_{prop}$ , and (c) Doppler shift in absolute value  $|f_d|$ . The  $SE$  is shown for a low ( $p=50\%$ ) and a high ( $p=0.001\%$ ) atmospheric attenuation. For  $t_{prop}$ , the time instances when handovers are performed are marked for Closest Satellite HO ( $\times$ ) and Max Visibility HO ( $\circ$ ). The handovers performed for Closest Satellite HO and Max Visibility HO are the same regardless of the atmospheric attenuation.



**FIGURE 8.** Average handover rate  $\rho_{HO}$  for the standalone scenario and different HO strategies, for the considered MEO and HEO constellations.

to-ground link for a high atmospheric attenuation (i.e.  $SE=0$  bps/Hz), regardless of the HO strategy. Consequently, other solutions like increasing the transmit power or antenna

gain are needed to maintain connectivity in case of less likely strong atmospheric disturbances.

Overall, these  $SE$  results emphasize that MEO constellations like Mangata are sensitive to the HO strategy choice for the typical low atmospheric attenuation conditions and Pleiades HEO is sensitive to the HO strategy choice for less likely high atmospheric attenuation conditions. For both constellations, Closest Satellite HO is preferred to maintain a high  $SE$ .

**PROPAGATION DELAY & HO RATE**

Let us now consider the propagation delay  $t_{prop}$  of Mangata MEO and Pleiades in Fig. 7(b). For Mangata,  $t_{prop}$  varies

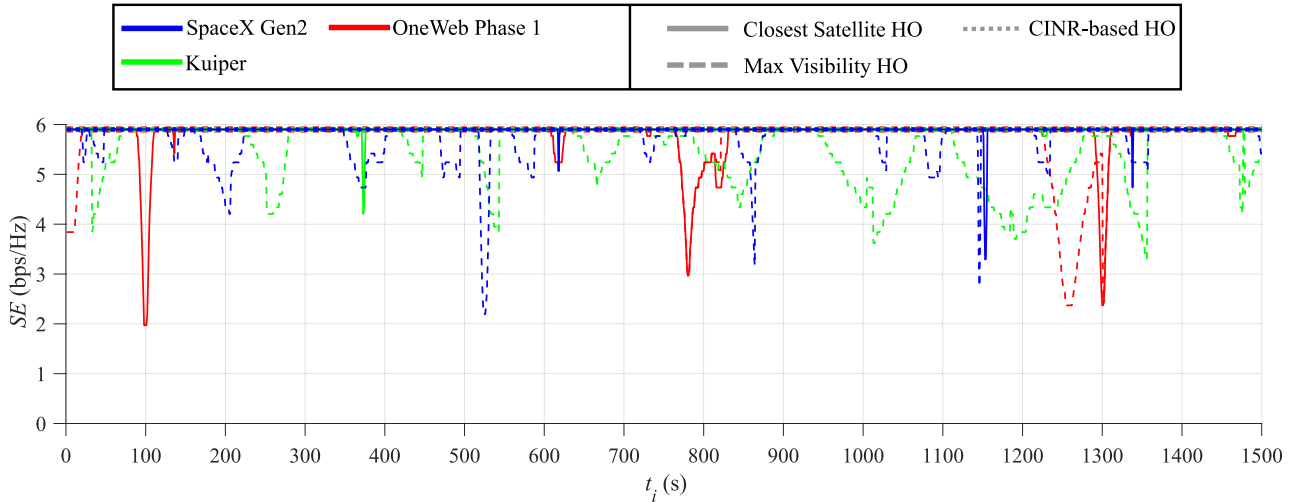


FIGURE 9. Link spectral efficiency  $SE$  over part of the simulated time  $t_i$ , for the inter-constellation interference scenario, for all considered HO strategies and private LEO constellations, for  $p=50\%$ .

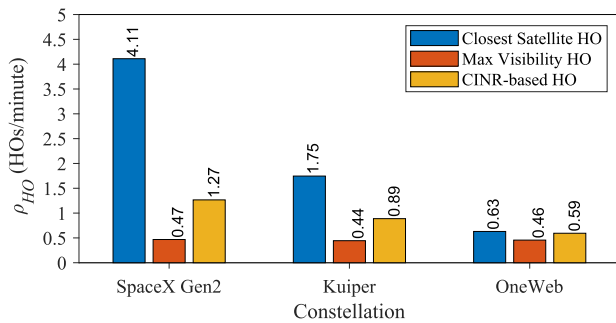


FIGURE 10. Average handover rate  $\rho_{HO}$ , for the inter-constellation interference scenario, for all HO strategies, the three considered private LEO constellations, and  $p=50\%$ .

from 20 to 30 ms, while for Pleiades  $t_{prop}$  is between 60 and 97 ms. These values correspond to the respective altitudes of Mangata (rather high) and Pleiades (very high). Importantly, for each of these two constellations, the choice of HO strategy has a significant impact on the delay. Specifically, the delay for Closest Satellite HO is lower than for Max Visibility HO by 10 and 20 ms for Mangata and Pleiades, respectively. This is a significant difference and confirms that Closest Satellite HO is a good choice for these constellations, from the point of view of the delay. We note that the same HO strategy was found useful for Mangata and Pleiades from the  $SE$  perspective.

Furthermore, the handover rate of these two constellations in Fig. 8 is rather low for both HO strategies, thus resulting in a low handover overhead. Namely, the difference between the upper and lower bounds is 0.14 HO/minute and 0.01 HO/minute for Mangata and Pleiades, respectively. This is due to the moderate to high altitude of the satellites, where each satellite has a large coverage area and thus a smaller constellation size is sufficient. For instance, for Pleiades there are four satellites visible at the ground station in Aachen at any given moment. We consider these differences between  $\rho_{HO}$  for different HO strategies to be

overall marginal, such that none of the HO strategies is preferred over the other from the perspective of the handover overhead, for MEO/HEO constellations.

DOPPLER SHIFT

We now discuss the Doppler shift  $f_d$  in Fig. 7(c). For Mangata MEO we observe that  $f_d$  is at most 35 kHz (1.84 ppm) for Closest Satellite HO, whereas for Max Visibility HO it is significantly higher, namely up to 166 kHz (8.74 ppm). This is due to the much larger range of angles  $\alpha$  that are covered by Max Visibility HO where the ground station keeps the connection to a satellite even at low elevation angles, jointly with the inclined orbits of Mangata. Our results thus suggest that Closest Satellite HO is preferable for Mangata MEO, since  $f_d$  is at most 1.84 ppm for this strategy and thus within the typical range achieved even after Doppler shift compensation [6]. This is consistent with the preferred HO strategy for Mangata MEO based on the other considered metrics.

The Doppler shift for Pleiades is overall low and varies over a small range for both Closest Satellite and Max Visibility, namely from 4 to 53 kHz (0.2 to 2.8 ppm). This is due to the high altitude at which Pleiades satellites become active, namely above 17118 km [4]. Thus,  $\alpha$  varies over a small range and also the velocity of the satellites above 17118 km is rather low for both HO strategies (from 2.3 to 3.8 km/h in our simulations). Consequently, the choice of HO strategy does not change the range of  $f_d$  for Pleiades.

SUMMARY

The results for the MEO and HEO constellations show overall that Closest Satellite HO is preferred for these types of constellations, due to its positive impact on  $SE$  and propagation delay, and the significant decrease in  $f_d$  for MEO constellations with inclined orbits.

**TABLE 5.** Summary of preferred HO strategy for all constellations, from the point of view of each metric, for the standalone scenario (S) and inter-constellation interference scenario (I).

Constellation \ Metric	SpaceX Gen2 LEO	Kuiper LEO	OneWeb Phase 1 LEO	Mangata MEO	Pleiades HEO
$SE$	S: Closest Satellite I: CINR-based	S: Closest Satellite I: CINR-based	S: Closest Satellite I: CINR-based	S: Closest Satellite I: CINR-based	S: Closest Satellite I: –
$t_{prop}$	S: Closest Satellite I: Closest Satellite	S: Closest Satellite I: Closest Satellite	S: Closest Satellite I: Closest Satellite	S: Closest Satellite I: Closest Satellite	S: Closest Satellite I: –
$\rho_{HO}$	S: Max Visibility I: Max Visibility	S: Max Visibility I: Max Visibility	S: any I: any	S: any I: any	S: any I: –
$f_d$	S: any I: any	S: any I: any	S: any I: any	S: Closest Satellite I: Closest Satellite	S: any I: –
Overall	S: CINR-based I: CINR-based	S: CINR-based I: CINR-based	S: Closest Satellite I: CINR-based	S: Closest Satellite I: CINR-based	S: Closest Satellite I: –

## B. INTER-CONSTELLATION INTERFERENCE SCENARIO

This section presents and discusses our results for the inter-constellation interference scenarios. We focus on the results for the three considered LEO constellations and we omit results for Mangata MEO and Pleiades HEO. This is since, in the inter-constellation interference scenario, we observed similar trends for Mangata MEO and the considered LEO constellations. Furthermore, Pleiades does not operate on the Ka-band channel with the highest number of operating constellations, which we assume in the inter-constellation interference scenario to obtain worst-case interference levels.

### 1) SPECTRAL EFFICIENCY

Fig. 9 shows the  $SE$  for the three considered LEO constellations, for all three HO strategies and a low atmospheric attenuation ( $p=50\%$ ). We observe that  $SE$  is most of the time close to the maximum of 6 bps/Hz, despite considering worst-case inter-constellation interference from all other co-channel constellations. This shows that inter-constellation interference does not have a major impact on  $SE$ , whereas, as observed in Section V-A, the atmospheric attenuation has a much stronger impact on  $SE$ . Furthermore, CINR-based HO achieves the maximum  $SE$  all the time, for all LEO constellations and protects them from sporadically high interference causing drops in  $SE$ . Thus, CINR-based HO is the most suitable for all LEO constellations, in order to achieve a high  $SE$ . Finally, we note that we observed the same trend for Mangata MEO, so we omit these results for brevity.

### 2) HO RATE, DELAY & DOPPLER SHIFT

Fig. 10 shows the handover rate  $\rho_{HO}$  for the inter-constellation interference scenario, for the three HO strategies and the considered LEO constellations, corresponding to the  $SE$  results in Fig. 9. We note that the results for Closest Satellite HO and Max Visibility HO are the same as those for the standalone scenario in Section V-A, for the respective constellations. This is expected, since with these two HO strategies the decisions to perform a handover are based on the constellation geometry and do not depend in any way on the inter-constellation interference. Furthermore, with CINR-based HO,  $\rho_{HO}$  takes different values for the

inter-constellation interference scenario compared with the standalone scenario, since for this HO strategy the decision to perform a handover is based on the CINR level and is thus affected by interference. Nonetheless, the trends with respect to the other HO strategies are the same, namely Max Visibility HO reduces significantly the handover overhead for SpaceX Gen2 and Kuiper, whereas for OneWeb Phase 1 all HO strategies result in a similar overhead.

Finally, we note that the results for the one-way propagation delay  $t_{prop}$  and Doppler shift  $f_d$  are overall within the same respective ranges as for the standalone scenario in Section V-A, since they are affected by the constellation geometry (altitude and inclination) and velocity, rather than the level of interference. Thus, for the sake of brevity, we omit the results for these metrics in the inter-constellation interference scenario.

## C. SUMMARY & DISCUSSION

We discuss our main findings and summarize the results in Table 5. The results for the standalone scenario showed that CINR-based HO is preferred for large LEO constellations like SpaceX Gen2 and Kuiper, since it achieves a good tradeoff between  $SE$ ,  $t_{prop}$ , and  $\rho_{HO}$ . By contrast, Closest Satellite HO is preferred for smaller polar LEO constellations like OneWeb, for which  $\rho_{HO}$  is less dominant (i.e. similar for all HO strategies), so  $SE$  and  $t_{prop}$  determine the handover strategy choice. Similarly, Closest Satellite HO is overall a good choice for MEO/HEO constellations, where the goal is to obtain a high  $SE$  and low delay, whereas the HO rate is less important since it is in any case low. Moreover, Closest Satellite HO limits the Doppler shift for Mangata MEO to low values.

Furthermore, we showed that the impact of the atmospheric attenuation on the space-to-ground link is dominant over the impact of inter-constellation interference. Nonetheless, CINR-based HO is useful to avoid sporadic strong interference, if interference mitigation techniques among different constellations are not in place. We emphasize that careful selection of the reference  $CINR_{max}$ , as we showed in Table 4, is required to obtain the desired behaviour and tradeoff among the considered metrics. This is since CINR varies highly with the atmospheric attenuation and unsuitable values

may result in no benefit over Closest Satellite HO or Max Visibility HO, which achieve the upper/lower bounds of the considered metrics. For instance, let's assume the case of a high atmospheric attenuation, where CINR typically has a low value. If the  $CINR_{max}$  reference value is configured as for a low atmospheric attenuation (namely with a high value), no CINR degradation will be tolerated at all and CINR-based HO will simply behave as Closest Satellite HO, trying to perform a handover as often as possible. In practice, this may require a learning phase to determine a suitable average reference value.

Overall, our results show that the communication performance and operation modes of the NGSO satellite constellations can be very different, so the optimal HO strategy depends on the constellation design and type. This suggests that the HO solutions for emerging satellite networks would have to be tuned according to the constellation specifics, potentially via adaptive algorithms for constellations that are being updated in time by adding new satellites and orbits with the same or different geometries. We note that this is rather common for private satellite operators, who recently updated their constellations several times, as illustrated by the different phases and generations of OneWeb and SpaceX in Table 1. Although studying explicitly constellation scalability design aspects is outside the scope of this paper, the different considered LEO constellations provide some initial scalability insights, since they span a wide range of sizes and thus reflect constellations that have an initial small deployment (OneWeb Phase 1) and are extended subsequently with more satellites (Kuiper), until becoming mega-constellations (SpaceX Gen2). Finally, we believe that our findings are relevant to satellite networks in general, namely private NGSO constellations, as considered in this study, as well as a valuable input to the design of future 3GPP-based NTN.

## VI. CONCLUSION

This paper presented an extensive study of the impact of inter-satellite HO strategies on the space-to-ground link performance. We selected three representative HO strategies, namely always connecting to the closest satellite (Closest Satellite HO), connecting to the maximum visibility satellite and remaining connected to it until it reaches the out-of-visibility range (Max Visibility HO), and performing a handover if CINR drops below a given threshold (CINR-based HO). The first two strategies achieved the upper and lower bounds of the spectral efficiency, delay, handover rate, and Doppler shift. Furthermore, with the third HO strategy handovers are performed in a way that avoids major drops in the spectral efficiency and also limits the number of handovers. We evaluated the impact of these HO strategies on five real emerging private NGSO constellations with different characteristics, i.e. SpaceX Gen2 LEO, Kuiper LEO, OneWeb Phase 1 LEO, Mangata MEO, and Pleiades HEO, where we assumed transmissions in the Ka-band to a ground station in Aachen. Furthermore, we considered two scenarios:

(i) standalone with perfect intra- and inter-constellation interference mitigation, and (ii) inter-constellation interference.

Our results showed that the optimal HO strategy depends on the constellation design, due to the very different spectral efficiency, delay, handover rate, and Doppler shift across the constellations. In the standalone scenario, CINR-based HO is recommended for large LEO constellations comprising thousands of satellites, to reduce less likely but significant decreases in the spectral efficiency due high atmospheric attenuation, while at the same time reduce the handover rate and associated overhead. For smaller LEO constellations with hundreds of satellites, Closest Satellite HO is preferred, since the handover rate is similar for all strategies, so the goal is to maximize the spectral efficiency and minimize the propagation delay. Furthermore, none of the HO strategies limits the Doppler shift to low values for LEO constellations. By contrast, Closest Satellite HO is always recommended for MEO and HEO constellations, since it achieves the highest spectral efficiency and lowest delay, which are critical given the long space-to-ground paths. Moreover, Closest Satellite HO achieves a low Doppler shift for Mangata MEO, while the handover rate is in any case low for the MEO and HEO constellations, due to their moderate to small sizes and high altitudes. In the inter-constellation interference scenario, the interference only seldom causes significant decreases in the spectral efficiency, but if the goal is to avoid such decreases at all, CINR-based HO is preferred. These results indicate overall that the choice of HO strategy for satellite networks should be adjusted based on the constellation type, design and interference conditions, for instance by means of adaptive algorithms, especially for constellations that are enhanced in time by adding new satellites and orbit types.

## REFERENCES

- [1] O. Kodheli, E. Lagunas, N. Maturo, S. K. Sharma, B. Shankar, J. F. M. Montoya, J. C. M. Duncan, D. Spano, S. Chatzinotas, S. Kisseleff, J. Querol, L. Lei, T. X. Vu, and G. Goussetis, "Satellite communications in the new space era: A survey and future challenges," *IEEE Commun. Surveys Tuts.*, vol. 23, no. 1, pp. 70–109, 1st Quart., 2021.
- [2] H. Tataria, M. Shafi, A. F. Molisch, M. Dohler, H. Sjöland, and F. Tufvesson, "6G wireless systems: Vision, requirements, challenges, insights, and opportunities," *Proc. IEEE*, vol. 109, no. 7, pp. 1166–1199, Jul. 2021.
- [3] P. Chowdhury, M. Atiquzzaman, and W. Ivancic, "Handover schemes in satellite networks: State-of-the-art and future research directions," *IEEE Commun. Surveys Tuts.*, vol. 8, no. 4, pp. 2–14, 4th Quart., 2006.
- [4] Federal Communications Commission (FCC). (Sep. 2023). *Schedule S*. [Online]. Available: <http://licensing.fcc.gov/cgi-bin/ws.exe/prod/ib/forms/reports/swr030b.hts?set=>
- [5] S. Tonkin and J. P. de Vries, "NewSpace spectrum sharing: Assessing interference risk and mitigations for new satellite constellations," in *Proc. TPRC*, Washington, DC, USA, Sep. 2018.
- [6] *Solutions for NR To Support Non-Terrestrial Networks (NTN)*, document TR 38.821, Version 16.1.0, 3GPP, May 2021.
- [7] G. Masini, P. Reininger, M. E. Jaafari, A. Vesely, N. Chuberre, B. Baudry, and J.-M. Houssin, "5G meets satellite: Non-terrestrial network architecture and 3GPP," *Int. J. Satell. Commun. Netw.*, vol. 41, no. 3, pp. 1–13, Jul. 2022.
- [8] E. Papapetrou, S. Karapantazis, G. Dimitriadis, and F. Pavlidou, "Satellite handover techniques for LEO networks," *Int. J. Satell. Commun. Netw.*, vol. 22, no. 2, pp. 231–245, Mar. 2004.

- [9] E. Papapetrou and F.-N. Pavlidou, "Analytic study of Doppler-based handover management in LEO satellite systems," in *Proc. IEEE Trans. Aerosp. Electron. Syst.*, Jul. 2005, vol. 41, no. 3, pp. 830–839.
- [10] M. Gkizeli, R. Tafazolli, and B. G. Evans, "Hybrid channel adaptive handover scheme for non-GEO satellite diversity based systems," *IEEE Commun. Lett.*, vol. 5, no. 7, pp. 284–286, Jul. 2001.
- [11] X. Hu, H. Song, S. Liu, and W. Wang, "Velocity-aware handover prediction in LEO satellite communication networks," *Int. J. Satell. Commun. Netw.*, vol. 36, no. 6, pp. 451–459, Nov. 2018.
- [12] B. Yang, Y. Wu, X. Chu, and G. Song, "Seamless handover in software-defined satellite networking," *IEEE Commun. Lett.*, vol. 20, no. 9, pp. 1768–1771, Sep. 2016.
- [13] S. He, T. Wang, and S. Wang, "Load-aware satellite handover strategy based on multi-agent reinforcement learning," in *Proc. IEEE Global Commun. Conf. (GLOBECOM)*, Dec. 2020, pp. 1–6.
- [14] J. Li, K. Xue, J. Liu, and Y. Zhang, "A user-centric handover scheme for ultra-dense LEO satellite networks," *IEEE Wireless Commun. Lett.*, vol. 9, no. 11, pp. 1904–1908, Nov. 2020.
- [15] C. Braun, A. M. Voicu, L. Simic, and P. Mähönen, "Should we worry about interference in emerging dense NGSO satellite constellations?" in *Proc. IEEE Int. Symp. Dyn. Spectr. Access Netw. (DySPAN)*, Newark, NJ, USA, Nov. 2019, pp. 1–10.
- [16] A. Guidotti, A. Vanelli-Coralli, T. Foggi, G. Colavolpe, M. Caus, J. Bas, S. Cioni, and A. Modenini, "LTE-based satellite communications in LEO mega-constellations," *Int. J. Satell. Commun. Netw.*, vol. 37, no. 4, pp. 316–330, Jul. 2019.
- [17] H.-L. Maattanen, B. Hofstrom, S. Euler, J. Sedin, X. Lin, O. Liberg, G. Masini, and M. Israelsson, "5G NR communication over GEO or LEO satellite systems: 3GPP RAN higher layer standardization aspects," in *Proc. IEEE Global Commun. Conf. (GLOBECOM)*, Israel, Dec. 2019, pp. 1–6.
- [18] M. Handley, "Using ground relays for low-latency wide-area routing in megaconstellations," in *Proc. 18th ACM Workshop Hot Topics Netw.*, Princeton, NJ, USA, Nov. 2019, pp. 125–132.
- [19] *Satellite Antenna Radiation Patterns for Non-Geostationary Orbit Satellite Antennas Operating in the Fixed-Satellite Service Below 30 GHz*, document Recommendation S.1528, ITU-R, 2001.
- [20] *Propagation Data and Prediction Methods Required for the Design of Earth-Space Telecommunication Systems*, document Rec. ITU-R P.618-13, Dec. 2017.
- [21] CNES (Centre National d'Études Spatiales). (2017). *ITU-R Propagation Models Software Library*. [Online]. Available: <https://logiciels.cnes.fr/en/node/33?type=desc>
- [22] *Second Generation Framing Structure, Channel Coding and Modulation Systems for Broadcasting, Interactive Services, News Gathering and Other Broadband Satellite Applications; Part 2: DVB-S2 Extensions (DVB-S2X)*, document A082-2 Rev. 2, Feb. 2021.
- [23] J. Suilmann, A. M. Voicu, L. Simic, and P. Mähönen, "The dense sky: Evaluating system coexistence of new NGSO satellite constellations in the Ka band," in *Proc. IEEE GLOBECOM Workshops (GC Wkshps)*, Madrid, Spain, Dec. 2021, pp. 1–6.



**ANDRA M. VOICU** received the B.Sc. degree in electronics and telecommunications engineering from the Politehnica University of Bucharest, in 2011, and the M.Sc. degree in communications engineering and the Ph.D. degree in electrical engineering and information technology from RWTH Aachen University, in 2013 and 2020, respectively. During the work in this article, she was a Postdoctoral Researcher with the Mobile Communications and Computing Group, RWTH Aachen University. Her research interests include mobile radio networks, spectrum sharing, and wireless technology standardization. She was a recipient of the IEEE International Symposium on Dynamic Spectrum Access Networks (DySPAN) Best Paper Award, in 2017.



**ABHIPSHITO BHATTACHARYA** received the B.Sc. degree in electronics and telecommunications from Jadavpur University, India, in 2015, and the M.Sc. degree in communications engineering from RWTH Aachen University, in 2021, where he is currently pursuing the Ph.D. degree with the Mobile Communications and Computing Group. His research interest includes satellite communications.



**MARINA PETROVA** (Member, IEEE) received the degree in electronics engineering and telecommunications from Ss. Cyril and Methodius University, Skopje, and the Ph.D. degree from RWTH Aachen University, Germany. She is currently a Professor of wireless communication with RWTH Aachen University and a Visiting Professor with the School of Electrical Engineering and Computer Science, KTH Royal Institute of Technology, Sweden. Her research interests include systems-level design of future intelligent wireless systems; mmWave and radar technologies; joint radio access; and mobile computing, modeling, optimization, and prototyping of protocols for wireless and mobile systems. She was a recipient of the Future Research Leader Award from the Swedish Foundation for Strategic Research and was named as a fellow of Wallenberg Academy in 2019. She served as an Editor for the IEEE WIRELESS COMMUNICATION LETTERS and IEEE TRANSACTIONS ON MOBILE COMPUTING.

• • •